A NEW FRC SOLUTION FOR A PARTIALLY PREFABRICATED INDUSTRIAL DECK

Marco di Prisco[1], Matteo Colombo[2], Kristof De Wilder[3] and Lucie Vandewalle[4]

[1] Professor, Politecnico di Milano, Department of Civil and Environmental Engineering, marco.diprisco@polimi.it
[2] Ass. Professor, Politecnico di Milano, Department of Civil and Environmental Engineering, matteo.colombo@polimi.it
[3] Postdoctoral researcher, KU Leuven, Department of Civil Engineering, kristof.dewilder@kuleuven.be
[4] Professor, KU Leuven, Department of Civil Engineering, lucie.vandewalle@kuleuven.be

ABSTRACT

A new prefabricated deck is introduced in an industrial building to propose a viable alternative to the classical TT deck with a R/C top slab cast in place. The solution is characterized by a bearing capacity of 10 kN/m^2, a main span of 14 m or more, an adjustable spacing in the orthogonal direction, FRC plates simply supported on the prestressed beams used as predalles, 4 cm thick, and a FRC top slab cast-in-place, 8 cm thick designed according to a continuous slab resting on the simply-supported beams. The proposed deck is a structural solution that tries to fit different issues like construction speed, transport cost reduction, structural optimization, high fire resistance (R120) and quality performance. All elements are made from SFRC with varying amounts of steel fibres. This paper firstly presents the concept of linearization to adequately select the necessary amount of fibres for the concrete mixtures used to cast the beams, predalles and top slab. Secondly, the results of the structural tests on four beams and two predalles are presented. The current design issues are highlighted and the validity of MC2010 equations in the case of multi-phase casting is verified. Two specific design situations for the precast beams are investigated: the shear behaviour at the support, where shear reinforcement is provided and prestressing action is only partially active, and far from the support, where only fibres are active, but the prestressing action is fully diffused and the web area is reduced due to holes allowing the passage of ducts and channels. Finally, a study is performed of the structural response of the composite system consisting of beams, predalles and a top slab cast-in-place.

Keywords: Steel fibre reinforced concrete, shear, industrial deck

Marco di Prisco, Full professor
Politecnico di Milano
Department of Civil and Environmental Engineering
Piazza Leonardo da Vinci 32, Edificio 5
20133 Milan
Italy

Email: marco.diprisco@polimi.it

1. INTRODUCTION

Steel Fiber Reinforced Concrete elevated slabs are an interesting design solution, because they can guarantee at the same time robustness, high construction speed, flexibility and economy, especially if combined with conventional reinforcement disposed only in limited zones [1]. This last concept allows the designer to use both a diffused reinforcement (fibres), valid at the same time for bending, shear and punching, and a concentrated reinforcement optimized in the alignment only in the critical zones where the crack propagation followed by localization requires an increased bending or shear resistance to face the effective loads at serviceability and ultimate limit states. The possibility to graduate the reinforcement in the structure is one of the main advantages of R/C structures, because it allows to better use the material resources and reduces the ductility requirements to reach the maximum bearing capacity of the whole structure. In the paper an industrial deck solution aimed at combining both the advantages of prefabrication and those of the cast-in-place solution is investigated. The classical TT elements are substituted by prestressed prefabricated 14m long beams, designed to reach a high fire resistance, and thin prefabricated plates (predalles) resting on the top chords of the beams, able to increase and adjust the beam spacing, reducing the transport costs without loosing the production speed. The final top slab cast in place guarantees a double way stiffness not only in its own plane, but also in bending, thus profiting of the slab redundancy. Starting from the material tuning, the paper describes the design strategy to guarantee the reliability of the new structural solution, following the Model Code approach [2,3,4,5].

2. MATERIAL CHARACTERIZATION AND SELECTION

2.1. Concept of linearization

In order to comply with the required FRC class requirements for the structural elements on one hand and to minimize the fibre content on the other hand, a number of standard displacement controlled three-point bending tests are performed on notched beams according to [4] with various amounts of fibre content but without changing the concrete matrix. Based on the obtained results, the characteristic values of f_{Rj} (with j=1,2,3,4) are determined assuming a log-normal distribution of the residual flexural tensile strength values. It is then assumed that the values of the residual flexural tensile strengths only depend on the fibre content if the concrete matrix does not change. Moreover, the variation of the residual flexural tensile strengths is assumed to vary linearly with respect to the fibre content. This approach allows the designer to accurately select the required fibre content for a certain FRC class with a limited amount of material tests. It was followed to determine the optimal fibre content to meet the FRC class requirements for both the beams and predalles (here referred to as Mixture 1) as well as the top slab (Mixture 2).

2.2. Preliminary tests for Mixture 1 – beams and predalles

The concrete mixture is presented in Table 1. Two different amounts of fibre content were assessed: 40 kg/m³ and 60 kg/m³. In total, 21 notched beams (12 for V_f equal to 40 kg/m³ and 9 for a fibre content of 60 kg/m³) were subjected to a standard three-point bending test according to [4]. Table 2 presents the obtained results for the flexural tensile strength $f_{ct,L}^{f}$ as well as the residual flexural tensile strengths $f_{R,j}$ (with j=1,2,3,4). The results in terms of nominal stress σ_N versus crack mouth opening displacement (CMOD) are shown in Figure 1a. Assuming a log-normal distribution of the residual flexural tensile strength, the characteristic values can be easily obtained. Figure 1 (b) presents the relationship between the residual flexural bending strengths f_{Rj} (with j=1,3) as a function of the amount of fibres. To obtain a FRC strength class 4c a minimum fibre dosage of 46 kg/m³ is required. The corresponding values of f_{R1k} and f_{R3k} are equal to 4.0 MPa and 3.8 MPa respectively thus meeting the 4c strength class requirements. The value 46 kg/m³ will be used in the construction phase. For testing purposes, the quantities 40 kg/m³ and 60 kg/m³ are maintained. The average cubic compressive strength is 57 MPa.

Table 1 Concrete mix composition for: beams and predalles **(**Mixture 1) and top layer slab (Mixture 2**)**

Mixture 1	**Amount [kg/m³]**	**Mixture 2**	**Amount [kg/m³]**
Cement CEM I 52.5R	380	Cement CEM IV/A 42.5R LH	470
Limestone filler	100		
Water SSD	190	Water SSD	188
Sand 0/4	620	Sand 0/4	1008
Mixed sand 0/12	440	Mixed sand 0/8	504
Coarse aggregates 8/15	710	Coarse aggregates 8/14	171
Superplasticizer	5.5 (slab) 7.0 (beam)	Superplasticer Shrinkage reducer	7.6 4.0
Steel fibres (Dramix 3D 65-60)	40-60	Steel fibres (Dramix 4D 65-60)	30/50/35
Polypropylene fibers	1.5 (slab) - 1.0 (beam)		

Table 2 Identified material properties of Mixture 1 for various amounts of fibre content

Mixture	**Parameter**	**Unit**	$f_{ct,L}^{f}$	$f_{R,1}$	$f_{R,2}$	$f_{R,3}$	$f_{R,4}$
Mixture 1 – 40 kg/m³	*N*	[-]	12	12	12	12	12
	mean	[MPa]	4.62	5.02	5.22	4.95	4.40
	st. dev.	[MPa]	0.63	1.31	1.48	1.36	1.24
	COV	[%]	13.63	26.11	28.26	27.49	28.17
Mixture 1 – 60 kg/m³	*N*	[-]	9	9	8	7	7
	mean	[MPa]	5.56	8.97	9.38	8.33	7.25
	st. dev.	[MPa]	0.65	1.46	1.28	1.30	1.30
	COV	[%]	11.65	16.22	13.68	15.58	17.94

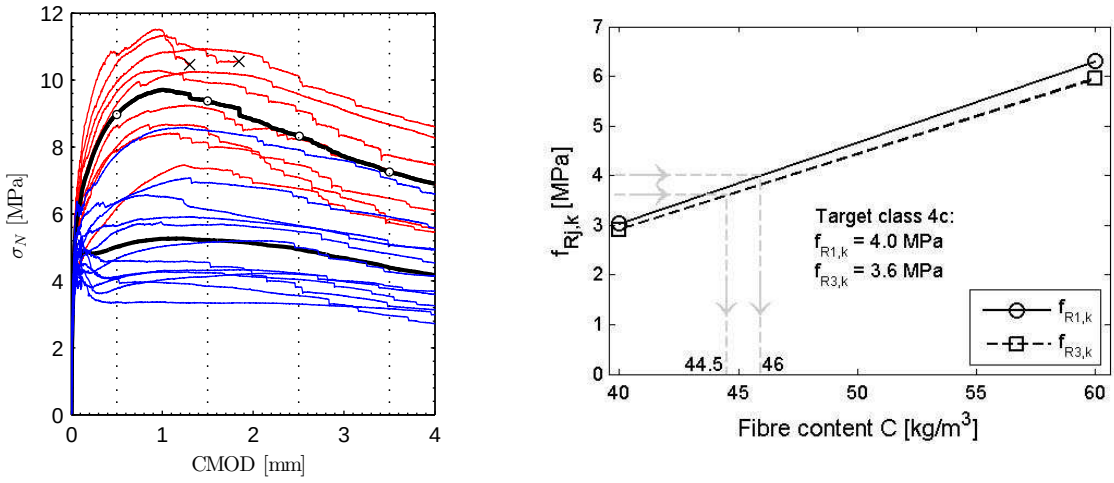

(a) (b)

Figure 1 Experimental results obtained from RILEM beam tests: (a) nominal stress versus CMOD for 40 kg/m³ (blue) and 60 kg/m³ (red) and mean curves (black); (b) linearization procedure for f_{R1} and f_{R3} (with indication of the minimum and maximum values (dotted lines) and mean value (dashed line)

2.3. Preliminary tests for Mixture 2 – top layer slab

The concrete mixture used to cast the top layer slab is also presented in Table 1. A similar approach as outlined above was followed to determine the optimal amount of fibres in the concrete mixture used to cast the top layer slab to obtain an FRC strength class 3c. Two different amounts of fibres were considered: 30 kg/m³ and 50 kg/m³. In total, 8 notched beams (5 for a fibre content of 30 kg/m³ and 3 in case of 50 kg/m³) were subjected to a standard three-point bending test [4]. Table 3 presents the

experimentally obtained results. The results in terms of nominal stress versus CMOD are depicted in Figure 2a. Similar to the results of Mixture 1, a log-normal distribution is assumed for the residual flexural bending strengths allowing for the determination of the characteristic values f_{R1k} and f_{R3k}. . Figure 1b presents the relationship between the residual flexural bending strengths f_{Rj} (with j=1,3) as a function of the amount of fibres. Figure 2b presents the relationship between the residual flexural bending strengths f_{Rj} (with j=1,3) as a function of the amount of fibres. To obtain an FRC strength class 3c a minimum fibre dosage of 33 kg/m³ is required. The corresponding values of f_{R1k} and f_{R3k} are equal to 3.0 MPa and 3.1 MPa respectively thus meeting the 3c strength class requirements. In order to verify this linearization procedure, 12 beams with 35 kg/m^3 of the same fibres were cast and tested at 28 days. The results of these tests are summarized in Table 3. The corresponding values of f_{R1k} and f_{R3k} are equal to 3.65 MPa and 3.74 MPa that allow us to classify the material as 3d thus indicating that the linearization procedure results in favour of safety. The cubic compressive strength of the material is 45 MPa.

Table 3 Identified material properties of Mixture 2 for various amounts of fibre content

Mixture	**Parameter**	**Unit**	$f_{ct,L}^{f}$	$f_{R,1}$	$f_{R,2}$	$f_{R,3}$	$f_{R,4}$
Mixture 2 – 30 kg/m³	*N*	[-]	5	5	5	5	5
	mean	[MPa]	4.23	3.90	4.92	4.62	2.51
	st. dev.	[MPa]	0.34	0.59	0.71	0.81	0.41
	COV	[%]	8.04	15.18	14.42	17.55	16.51
Mixture 2 – 50 kg/m³	*N*	[-]	3	3	3	3	3
	mean	[MPa]	4.61	8.16	9.51	7.74	6.39
	st. dev.	[MPa]	0.28	1.73	0.89	1.49	1.84
	COV	[%]	6.15	21.22	9.39	19.27	28.74
Mixture 2 – 35 kg/m³	*N*	[-]	12	12	12	12	12
	mean	[MPa]	5.24	5.92	7.41	5.20	3.28
	st. dev.	[MPa]	0.62	1.20	1.29	0.77	0.75
	COV	[%]	13.03	20.32	17.43	14.86	22.93

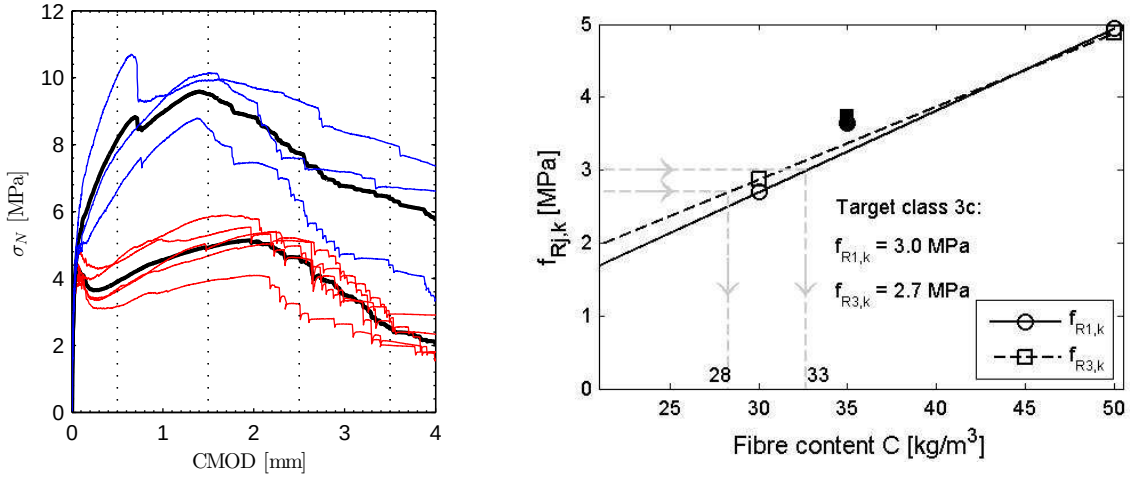

(a) (b)

Figure 2 Experimental results obtained from RILEM beam tests: (a) nominal stress versus CMOD for 30 kg/m³ (red) and 50 kg/m³ (blue) and mean curves (black); (b) linearization procedure for f_{R1} and f_{R3} (with indication of the minimum and maximum values (dotted lines) and mean value (dashed line)

3. BEAM TESTING AND DESIGN ISSUES

To ensure that the proposed design for the main bearing beams meets all the safety and serviceability requirements, four I-shaped beams (2 sets of two identical beams) were produced. Each specimen, characterized by an I-shaped cross section is 4500 mm long, 700 mm high. The upper and lower flange width is equal to 250 mm and 450 mm respectively whereas the thickness of the web is 150 mm. The fibre content of all specimens was equal to 60 kg/m³. Each specimen is prestressed using twelve 7-wire strands (nominal diameter 12.5 mm) at the bottom and one 7-wire strand (nominal diameter 12.5 mm) near the top of the beam. Each strand was given an initial prestressing force equal to 130.2 kN. Additionally, two non-prestressed 7-wire strands (nominal diameter 12.5 mm) and 3 bars (nominal diameter 14 mm) are provided at the bottom. Compressive reinforcement is provided at the top of each specimen consisting of seven bars (nominal diameter 24 mm) simulating the effect of the predalles and top layer slab. Casting of each specimen is performed in two phases to simulate the discontinuity of the final solution. Shear reinforcement was provided in all specimens and consisted of double-legged stirrups with a nominal diameter of 10 mm (center-to-center distance equal to 150 mm, 200 mm or 300 mm). Shear reinforcement was omitted in beams 1 and 2 over a distance equal to 1900 mm. Finally, a hole (diameter 150 mm) is cored in the web of specimens 1 and 2. Two specific design situations are assessed: (a) the shear behaviour at the support where the prestressing action is only partially active and (b) the shear behaviour far from the support where the prestressing force is fully developed, but circular openings in the web exist. In the following, each design situation is analyzed seperately. Firstly, the experimental setup is presented, Secondly, the full-scale results are reported. Finally, design issues and MC2010 shortcomings are highlighted.

3.1. Beams 3-4: shear behaviour near an end zone

3.1.1. Experimental set-up

Both specimens are subjected to a displacement-controlled three-point bending test using an electro-mechanical press (maximum capacity of press assembly: 1 MN). The applied displacement was monotonically increased at a constant displacement rate. The initial displacement rate was equal to 50 μm/s and was increased to 60-100 μm/s at higher load levels. A steel transfer beam is used to impose the applied displacement. A schematic representation of the experimental setup is shown in Figure 3. Among other instrumentation, five displacement transducers, labelled LVDT 1-5, were used to monitor the vertical displacement of the test specimen during the loading procedure.

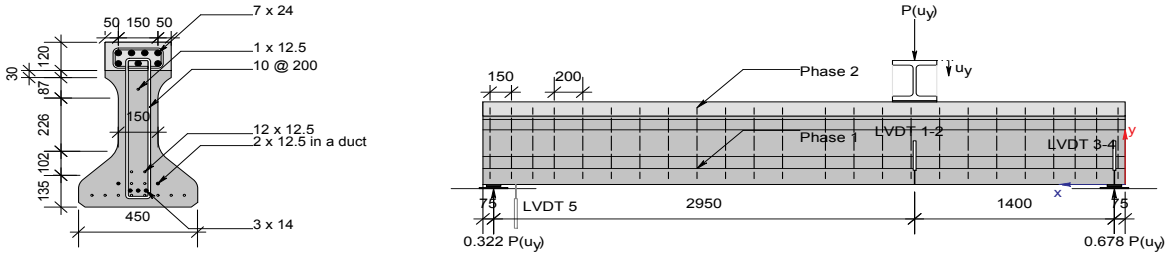

(a) (b)

Figure 3 Schematic representation of (a) cross section and (b) experimental setup of beams 3 and 4

3.1.2. Full-scale experimental results

The full-scale experimental results in terms of load-displacement response (both global data, obtained from the load-stroke from the press, and local data, obtained from the LVDTs), cracking pattern and failure mode are presented in Figure 4, Figure 5 and Figure 6 respectively. It must be noted that only partial data from Beam 3 and no data of Beam 4 are presented in Figure 4b due to the fact that the LVDTs lost contact with the test specimen early on during the loading procedure.

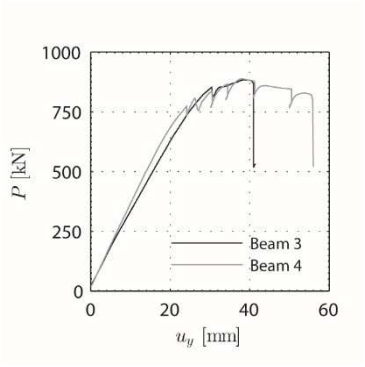

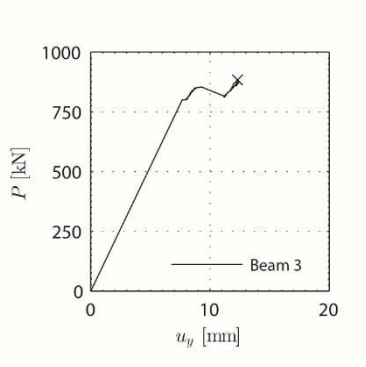

(a) (b)

Figure 4 Load displacement reponse for beams 3 and 4: (a) global behaviour obtained from the load-stroke data of the press; (b) local behaviour obtained from the LVDTs

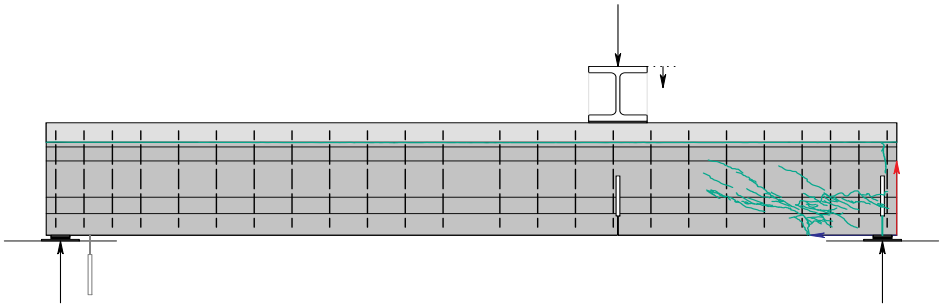

(a)

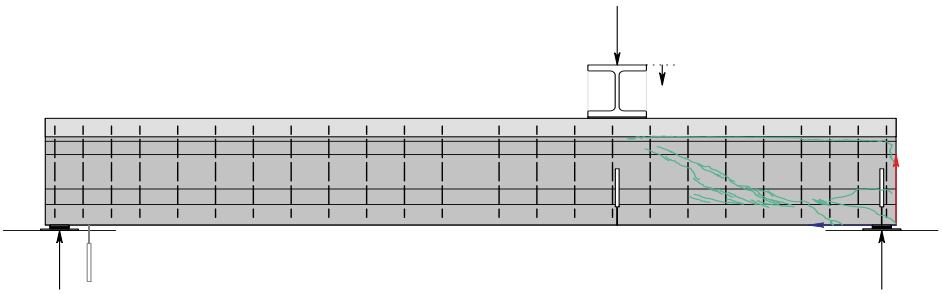

(b)

Figure 5 Experimentally observed cracking pattern prior to failure for specimens (a) Beam 3 and (b) Beam 4

(a) shear failure Beam 4 (b) strand penetration Beam 3

Figure 6 Failure modes observed and damage mechanisms for Beams 3 and 4

Figure 4a cleary indicates that both specimens exhibited a ductile behaviour. After the onset of inclined web cracking, a significant post-cracking behaviour is noticeable. Apart from numerous web cracks, sliding between the top and bottom cast phases was observed together with debonding of the prestressing strands, refer to Figure 6b. The loads at which inclined cracking was initiated P_{cr} as well as the maximum load P_u are presented in Table 4.

3.1.3. Design issues

Current design procedures for FRC structural elements found in MC2010 allow for the quantification of the initial web cracking load as well as the determination of the ultimate bearing capacity. The initial web cracking load P_{cr} can be determined using Equation (1)**.**

$$\boldsymbol{P_{cr} = \frac{\sqrt{\left(f_{ctk}+\frac{\sigma_{cp}}{2}\right)^2-\left(\frac{\sigma_{cp}}{2}\right)^2}\, b_w z - V_{sw}}{0.678}} \quad (1)$$

In Equation (1), f_{ctk} is the characteristic uni-axial tensile strength which can be derived from the average value of the limit of proportionality multiplied by a factor 0.7. According to Ferrara & di Prisco [6], the value of the uni-axial tensile strength can be taken equal to 90% of the limit of proportionality determined from notched specimens. Here, the values of f_{ctk} were found to be equal to 2.82 MPa and 3.01 MPa for the two slabs cast in two batches, characterized respectively with 6 and 5 specimens. The web width b_w is equal to 150 mm whereas the internal lever arm can be taken equal to 560 mm (80% of the total height). The value of the mean normal stress due to the applied prestressing force σ_{cp} depends on the location along the beam since the prestressing force requires a certain development length. Taking into account 20% prestress losses with respect to the initial stress due to immediate and time-dependent stress losses as well as the required development length of the prestressing force, a value of σ_{cp} equal to 7.50 MPa was found in the middle of the shear span. Finally, V_{sw} represents the shear force in the middle of the shear span due to the self-weight of the beam. The results of the above outlined calculation procedure are presented in Table 4.

Table 4 Experimentally observed and theoretically calculated cracking and failure loads for Beams 3 and 4

Specimen	$P_{cr,exp}$	$P_{cr,calc}$	$P_{cr,exp}/P_{cr,calc}$	$P_{u,exp}$	Failure	$P_{u,calc}$	$P_{u,exp}/P_{u,calc}$
	[kN]	[kN]	[-]	[kN]	mode	[kN]	[-]
Beam 3	847.1	818.7	1.03	884.6	S+A	724.0	1.22
Beam 4	764.8	818.7	0.93	888.7	S+A	724.0	1.23

Note: S+A indicates combined shear failure with loss of Anchorage

According to MC2010 [5] the ultimate shear capacity of an FRC structural element with both fibres and conventional shear reinforcement can be determined from Equation (2).

$$\boldsymbol{V_R = \frac{A_{sw}}{s} z f_{ywd} \cot\theta + \left[0.18\left(1+\sqrt{\frac{200}{d}}\right)\left[100\rho_l\left(1+7.5\frac{f_{Ftuk}}{f_{ctk}}\right)f_{ck}\right]^{\frac{1}{3}} + 0.15\sigma_{cp}\right] b_w d} \quad (2)$$

In Equation (2), A_{sw}/s represents the area of shear reinforcement per unit length, f_{ywd} is the yield stress of the shear reinforcement and θ denotes the angle measured between the inclined compressive stress field with respect to the horizontal. Depending on the adopted level of approximation (LOA), the aforementioned angle can take different values. Adopting the first LOA, the value of θ is equal to 25°. Moreover, d denotes the effective depth equal to 620 mm and f_{Ftuk} is the characteristic value of the ultimate residual strength, taken equal to $f_{R3k}/3$. The result of the evaluation of the above mentioned equation is presented in Table 4. An underestimation of the failure load is found. Since the applied load is relatively close to the support, a contribution of arch action could be the reason for this discrepancy.

3.2. Beams 1-2: shear behaviour in beams with reduced web area due to a hole

3.2.1. Experimental setup

Similar to beams 3 and 4, specimens 1 and 2 were subjected to a displacement-controlled three-point bending test. Five displacement transducers, labelled LVDT 1-5, were used to continuously monitor the vertical deflection at the location of the supports and the point load. Two inclined displacement transducers, labelled T1-2, were placed at 45° in the web to measure the tensile deformation around the circular hole. The applied displacement rate was equal as for specimens 3 and 4. A schematic representation of the adopted experimental setup is show in Figure 7.

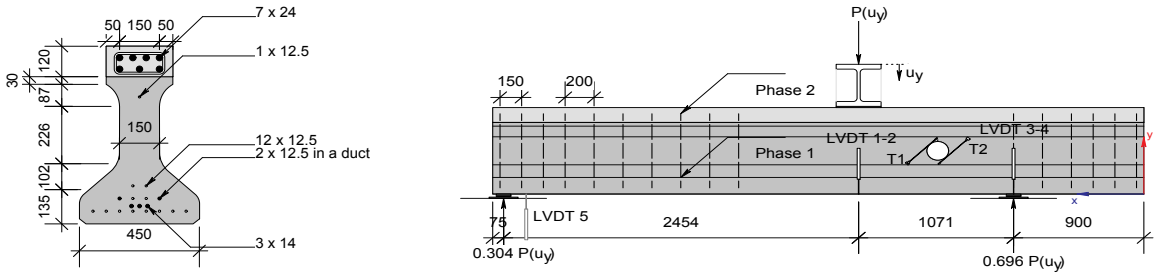

(a) (b)

Figure 7 Schematic representation of (a) cross section and (b) the experimental setup for beams 1 and 2

3.2.2. Full-scale experimental results

The experimental results in terms of load-displacement response, cracking pattern and failure mode for specimens without shear reinforcement and characterized by a reduced web area due to a hole are presented in Figure 8, Figure 9 and Figure 10.

Figure 8a,b clearly shows that Beams 1 and 2 exhibited a highly brittle behaviour near failure in comparison to the results of Beams 3 and 4 presented in Figure 4(a-b). Small inclined cracks originating from the edge of the hole were observable early on during the loading procedure. Increasing the applied displacement and thus the applied load led to a further development of the cracking pattern. Despite the aforementioned cracking pattern, the behaviour remained nearly perfectly linear elastic until the maximum load (824.4 kN and 903.6 kN for beams 1 and 2 respectively). Similar to Beams 3 and Beam 4, sliding between the two cast phases was observed as shown in Figure 10b.

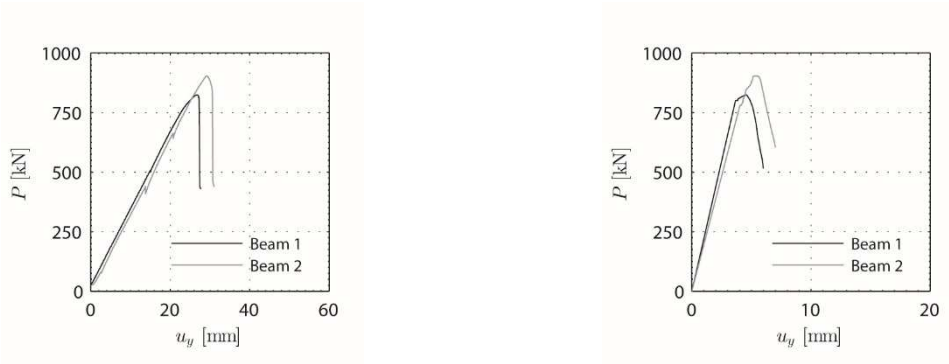

(a) (b)

Figure 8 Load displacement reponse for beams 1 and 2: (a) global behaviour obtained from the load-stroke data of the press; (b) local behaviour obtained from the LVDTs

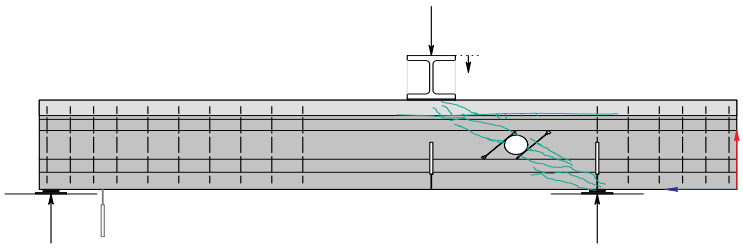

(a)

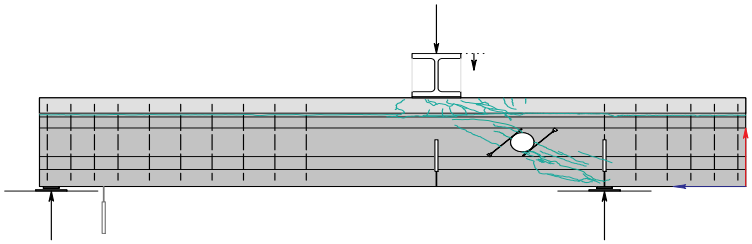

(b)

Figure 9 Experimentally observed cracking pattern prior to failure for (a) Beam 1 and (b) Beam 2

(a) (b)

Figure 10 Typical failure modes and damage mechanisms for Beam 1 and Beam 2

3.2.3. Design issues

Although the geometry of Beams 1 and 2 is frequently observed in practice, practical guidelines for the design of these members, especially in fibre reinforced concrete, are absent. To better understand the behaviour of such beams, numerical simulations have to be performed. This paper presents the results of a straightforward linear analysis to better understand the stress state around the circular hole which leads to initial cracking. A phase plane stress model with quadratic quadrilateral elements was therefore developed in the commercially available software DIANA. Firstly, the prestressing force is applied on the bottom part (first cast phase). Onto this stress state, that due to self-weight and a certain load is superimposed. For both Beams 1 and 2, inclined cracks were visible at 250 kN (Crack 1) and 280 kN (Crack 2), refer to Figure 11 where clear nonlinear behaviour is observed at the aforementioned loads. Rather than applying a certain displacement to the model, these loads were selected and applied onto the numerical model. The stress state in terms of principal tensile stress σ_1 expressed in polar coordinates is assessed. The results are presented in Figure 12.

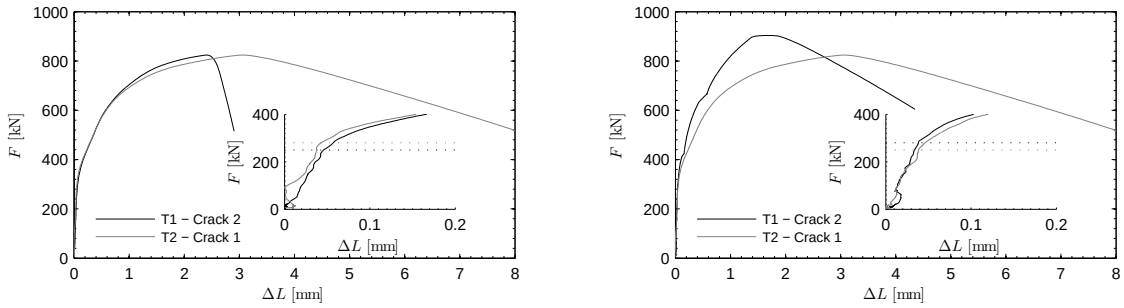

(a) (b)

Figure 11 Measured displacements of T1 and T2, refer to Figure 7 for (a) Beam 1 and (b) Beam 2

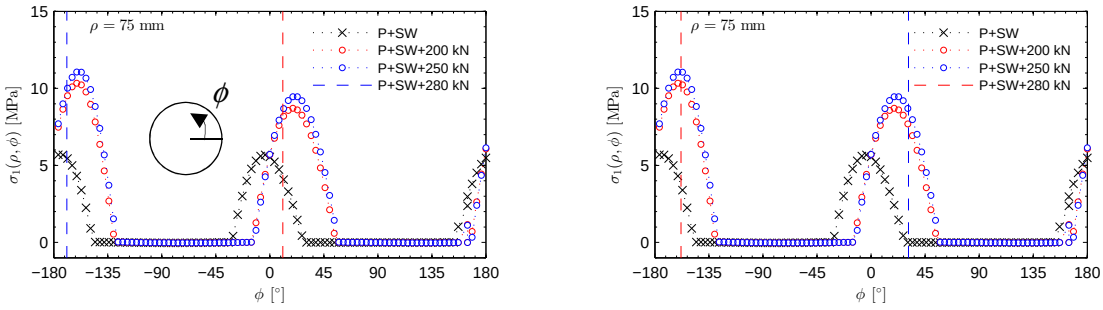

(a) (b)

Figure 12 Principal tensile stress state around the edge of the hole at various load levels (only Self Weight (SW), SW+250 kN and SW+280 kN) with indication of the experimentally observed angle of for (a) Beam 1 and (b) Beam 2

The aforementioned Figure 12 presents the value of the principal tensile stress, obtained from a purely elastic analysis (hence the unrealistically high stress values), as a function of the angle ϕ measured counter clockwise with respect to the horizontal, refer to Figure 12a, as a function of the applied load. The experimentally observed angle along the edge of the hole where cracking was initiated is also indicated in a dashed line from which the colour corresponds to the load at which the crack occurred. From Figure 12, it can be concluded that a good correspondence is found between the experimentally observed location of crack initiation and the results of the linear FE model. However, to accurately predict the actual cracking load and to understand the post-cracking behaviour a detailed nonlinear numerical model is required. Further research will focus on the development and analysis of an advanced nonlinear numerical model.

4. PREDALLES TESTING AND DESIGN ISSUES

The proposed structural solution consists of prefabricated prestressed SFRC beams on which SFRC precast slabs are placed, used as predalles. To ensure safety during the construction phase as well as during the service life, two precast SFRC predalles (length 1540 mm, width 1000 mm) are tested, labelled slabs 1 and 2. The initial cracking load, the load required to obtain buckling of the top reinforcement bars and the residual bearing capacity are determined and compared to analytical calculations. The predalles are prefabricated using the concrete mixture presented in Table 1 (Fiber content equal to 40 kg/m³, V_f = 0,51%).

4.1. Experimental setup

Two simply supported predalles are subjected to a displacement-controlled four-point bending test using an electro-mechanical press (maximum capacity 1 MN of press assembly) as shown in Figure 13. The applied displacement from the press is converted to four point loads using steel transfer

beams. Four load cells resting on concrete cubes (150x150x150 mm³) were provided to accurately monitor the corresponding force at each loading point. A schematic representation of the experimental setup is shown in Figure 14. The slab itself is 40 mm thick and provided with 6 bars (diameter 5 mm, centred 10 mm from the top of the slab). Thee top-chord bars (diameter 7 mm) of the 3 welded steel trusses are kept outside the slab (Figure 14b). The distance between two consecutive welded joints of the top reinforcement bars is equal to 200 mm.

(a) (b)

Figure 13 Experimental setup of predalles: (a) overview; (b) detail of load cells mounted on cubes

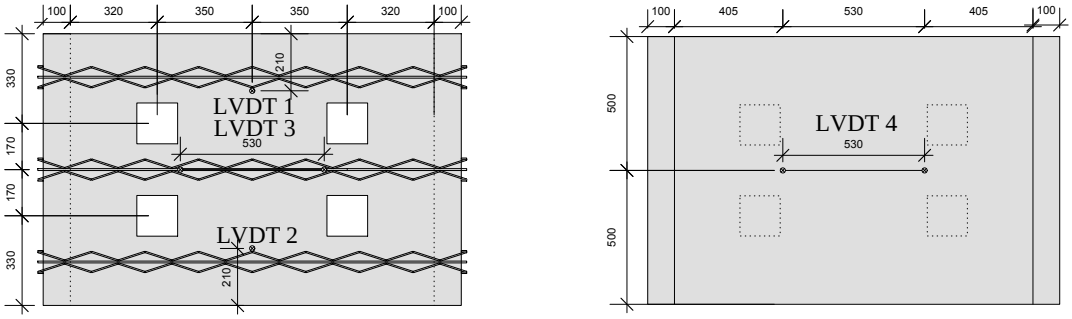

(a) (b)

Figure 14 Schematic representation of the experimental setup of the predalles: (a) top view; (b) bottom view

Apart from the aforementioned load cells, four displacement transducers were provided, labelled LVDT 1-4. LVDT 1 and 2 measured the vertical displacement near the outside of the slab, refer to Figure 14a. Two additional LVDTs were provided to measure the horizontal deformation at the top and bottom of the slab. The applied displacement rate was equal to 50 µm/s.

4.2. Experimental results

The experimentally observed load-displacement response, obtained from the average of both LVDT 1-2, for both slabs is presented in Figure 15. The presented load is the sum of the four load cells. The behaviour of both slabs is nearly identical. Firstly, the slab exhibits bending cracks. Shortly after, buckling of the top reinforcement bars is observed. Finally, the displacement is furthermore increased until the test is stopped due to excessive mid-span displacement and significantly reduced bearing capacity. The failure modes of both specimens are presented in Figure 16. The loads at which cracking and failure were observed are presented in Table 5.

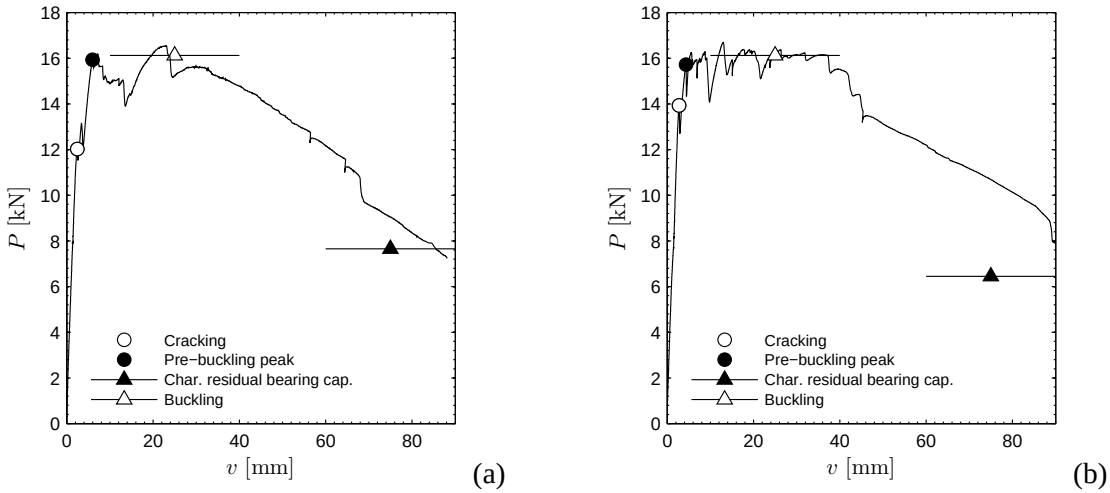

Figure 15 Experimentally observed load-displacement response for (a) Slab 1; (b) Slab 2 with indication of the results of the analytical calculations, refer to Section 4.3

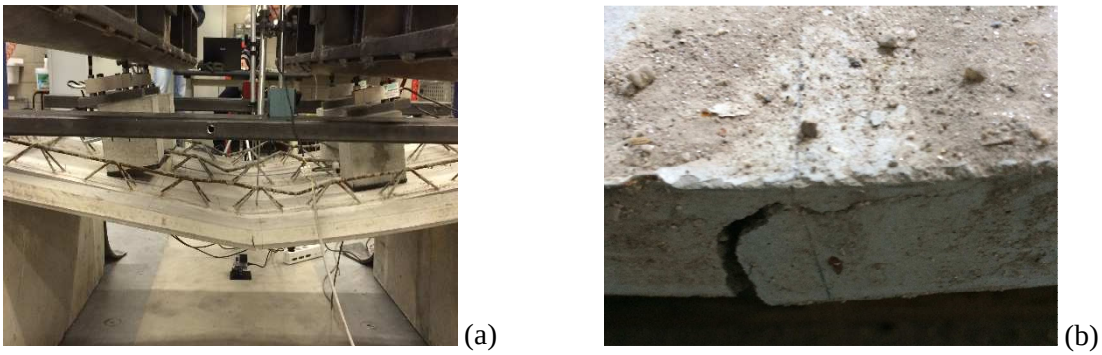

Figure 16 Failure modes of the predalles: (a) general deformed shape; (b) detail of midspan crack

Table 5 Experimentally observed cracking and buckling load compared to theoretical calculations

Specimen	**Cracking**			**Buckling**
	$P_{cr,exp}$	$P_{cr,calc,k}$	$P_{cr,exp}/P_{cr,calc,k}$	$P_{buckl,exp}$
	[kN]	[kN]	[-]	[kN]
Slab 1	12.05	12.61	0.96	16.01
Slab 2	13.93	12.74	1.09	16.00

4.3. Design issues

This sections analyses the three main stages of the experimentally observed behaviour: cracking, buckling of the top reinforcement bars and the post-buckling residual bearing capacity.

4.3.1. Cracking load

The load at which cracking is to be expected can be easily determined based on the theory of elasticity by considering a composite section. The main unknown is the flexural tensile strength of thin slab, $f_{ct,fl}^{40}$. Therefore, the uni-axial average tensile strength f_{ct} is firstly determined as 90% [6] of the limit of proportionality $(f_{ct,L}{}^{f})_{,m}$ determined on notched specimens. Secondly, the flexural tensile strength of a thin slab is determined accounting for stress redistribution over the cross section, refer to Equation (3) (with h equal to 40 mm).

$$\boldsymbol{f_{ct,fl}^{40} = \alpha_{fl}^{-1} f_{ct} = \frac{1+0.06h^{0.7}}{0.06h^{0.7}} 0.9 f_{ct,L}^{f}} \tag{3}$$

Given the loading geometry, the load at which cracking is to be expected can be determined using Equation (4) (where units [N,mm] should be used).

$$P_{cr,calc} = 2\frac{\frac{f_{ct,fl}^{40} I_0}{y_0} - M_{sw}}{a} \quad (4)$$

In Equation (4), I_0 represents the second moment of area of the transformed composite section whereas y_0 denotes the distance from the neutral axis to the most tensioned fibre and a is the load lever arm. The effect of the self-weight of the slab at the location of the maximum moment due to the applied load is taken into account via the term M_{sw}. The results of the aforementioned calculation procedure, where the characteristic value of $f_{ct,fl}^{40}$ is used, are presented in Table 5: a reasonable comparison is obtained.

4.3.2. Buckling load

To determine the load at which buckling of the top reinforcement bars is expected, knowledge of the buckling length $l_0=\alpha L$ (with L the length between two consecutive welds, equal to 200 mm) is required. The buckling length is function of the rotational stiffness at the location of the weld. Since this is unknown, a reverse identification procedure is adopted based on the obtained experimental results. Given the fact that buckling of the top reinforcement bars occurred at a load P approximately equal to 16 kN, the value of α can be determined based on Equation (5) (where units in [N, mm] should be used).

$$\alpha = \frac{1}{L}\sqrt{\frac{3\pi^2 EIz}{aP/2+M_{sw}}} \quad (5)$$

In Equation (5), the modulus of elasticity E is equal to 204 GPa whereas the second moment of area I of one bar is equal to $\pi 3.5^4/4$. The internal lever arm z between the centre of the top reinforcement bars and the resultant of the tensile stresses is here taken equal to 63 mm. The load P is the value of each point load, thus approximately equal to 4000 N. Evaluating Equation (5) results in a value for α equal to 0.61. Thus it can be concluded that welding the top reinforcement bars approximately results in two quasi-clamped boundary conditions.

4.3.3. Post-buckling residual bearing capacity

After buckling, the residual bearing capacity can be determined by taking only the bottom cracked slab into account and thus neglecting the influence of the buckled top bars. Assuming a linear-perfectly plastic constitutive model for the internal reinforcement bars, the ultimate limit state in bending is obtained when either the compressive strain reaches its maximum value ε_{cu} or the strain at the bottom of the slab reaches the maximum value ε_{Fu}. The latter is equal to the minimum of $2\cdot10^{-2}$ or the strain required to obtain a crack width of 2.5 mm. For the latter, the value of the characteristic length has to be known. Since the slab is relatively thin, the characteristic length is also small. Hence, the strain to obtain a crack width of 2.5 mm highly exceeds $2\cdot10^{-2}$. Thus the maximum allowable strain in the presented case is $2\cdot10^{-2}$. A simplified stress-strain relationship for concrete (using a block stress diagram over a height λx) is adopted whereas a rigid plastic model for FRC is adopted (with $f_{Ftu}=f_{R3}/3$). Based on horizontal equilibrium, the depth of the neutral axis is determined satisfying the strain compatibility conditions. The residual bending moment follows from rotational equilibrium. The characteristic values of f_{Ftu} are used: the results are presented in Figure 15. A good agreement was found between the experimental results and the analytically calculated post-buckling bearing capacity.

5. COMPOSITE SYSTEM: BEAM, PREDALLES AND TOP SLAB

Finally, the solution proposed for the composite system has been also tested in order to investigate the transverse behaviour of the floor when supported over the beams. To reproduce such situation, a statically redundant static scheme was adopted for the test by considering the slab supported over three points as shown in Figure 17a. Three 25 cm x 25 cm columns were used to simulate the beams heads over which predalles are simply supported; three closed loop B 450A stirrups with a diameter

of 10 mm protruded from the top surface to reproduce the real connection in the zone with the minimum number of connection. A 8 cm thick SFRC layer made by the material previously denoted as Mixture 2 was cast over the top of the predalles and a Φ6 20cmx20cm steel mesh was placed over the stirrups on the central support for a length of 80cm to resist the negative bending moment. The elements tested had a width of 1m. In order to compute the bending moment distribution over the structure, the reaction force over the central support was measured by means of two load cells.

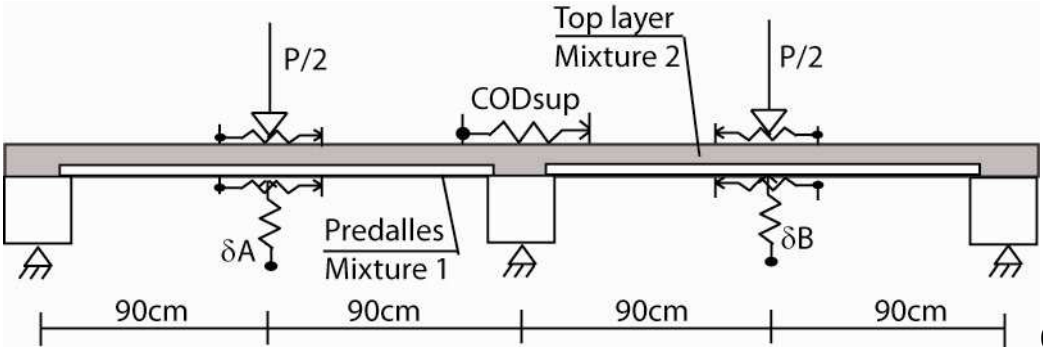

(a)

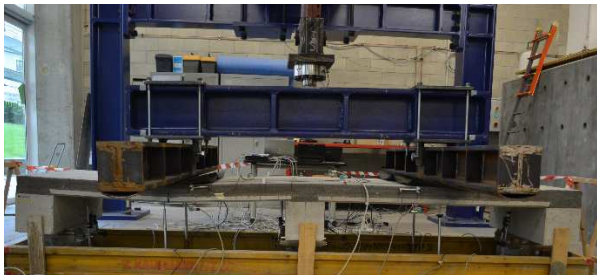

(b)

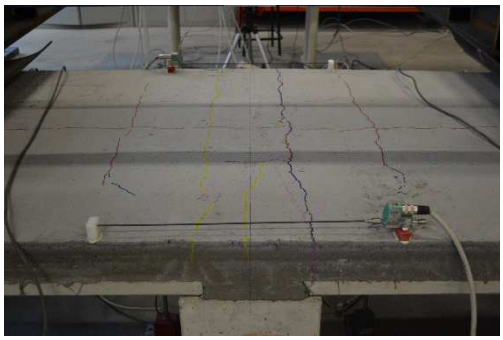

(c)

Figure 17 Test on composite solution: (a) loading scheme (b) specimen and failure and (c) crack pattern over the central support

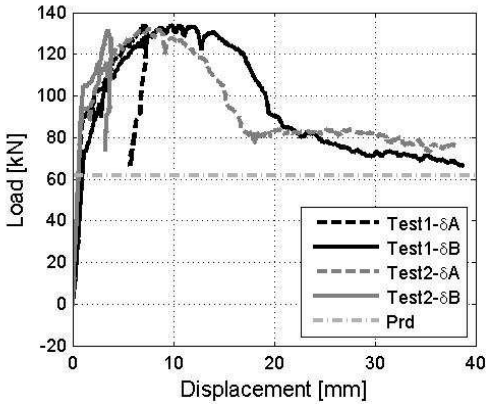

(a)

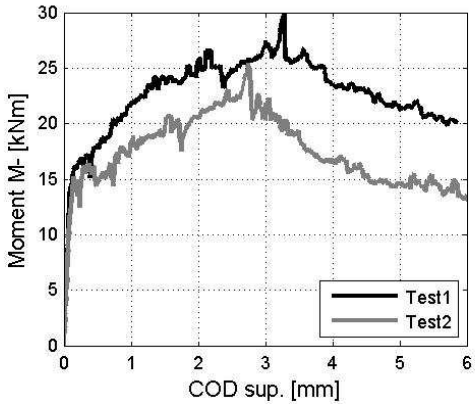

(b)

Figure 18 Test results on composite solution: (a) load vs displacement curve (b) negative bending moment over the support vs crack opening displacement

Two nominally identical test were carried out and Figure 17b and c show pictures of the test with the specimen at failure. It is worth to note that during the tests just one of the cross section at mid-span (right for test 1 and left for test 2) experiences crack localization that drives the global failure of the structure: the unloading of the vertical displacement under the other load knife can be followed in Figure 18a for both the tests. The test results are reported in Figure 18a and b respectively in terms of load (P) versus mid-span displacements curves for both the spans (δA and δB) and in terms of

negative bending moment (M-) over the support vs. crack opening displacement at the extrados over the support. In Figure 18a the dashed horizontal line corresponds to the maximum design load computed starting from the material class 3c with γ_F =1.5, the steel properties f_{yd} = 391 MPa con γ_s =1.15, without any sliding between the prefab slab and the cast in place layer, and using redistribution associated to the limit analysis with K_{Rd} = 1, corresponding to the reaching of the ultimate design bending moment in two plastic hinges (M^+ = 9.01 kNm and M^- = 9.66 kNm). The ultimate bending moments are computed by adopting a linear model approach arrested at w_u = 2.5 mm, according to Model Code [5]. It is significant to underline that the ultimate load corresponding to the reaching of the ultimate bending moment only in the central support corresponds in this case to P_u = 57.24 kNm instead of 61.05 kNm with an increase due to redistribution of only 6.6%.

6. CONCLUSIONS

A new solution for industrial deck adopting SFRC is presented. It proposes prefabricated and cast in place elements. The main tests carried out to calibrate the material performance and verify the reliability of the design approach used, following the Model Code 2010, are presented. The equations related to bending of thin slabs, composite deck and shear for prestressed beams offer a safety coefficient always larger than the required values. The ductility of the deck in the real situation is much larger than that measured in the tests, because it could use a full 2-way bending resistance, even if the behaviour expected is orthotropic. The only problem found concernes the shrinkage. In order to reduce it, the final solution adopted a cement content of 380 kg/m^3, 100 kg/m^3 of limestone filler and a special care of the surface treatment to prevent the loss of water in the first week.

ACKNOWLEDGMENTS

The Research Foundation Flanders (FWO) is gratefully acknowledged for the financial support provided to the third author by means of a long-term travel grant (Grant number V401516N).

The research has been financially supported by Sterline Company. Magnetti and Finazzi production companies and DSC-Erba design company are also acknowledged for the preparation of the specimens and their contribution in the definition of the variable parameters.

REFERENCES

1. di Prisco, M., Plizzari, G., Vandewalle, L. (2014) Structural design according to fib MC 2010: comparison between RC and FRC elements. In FRC 2014 Joint ACI-fib International Workshop - Fibre Reinforced Concrete: from Design to Structural Applications, Editors: Charron J.P., Massicotte B. , Mobasher B., Plizzari G., Montreal, Canada.
2. di Prisco, M., Plizzari, G., Vandewalle, L. (2009) Fibre reinforced concrete: New design perspectives, Materials and Structures/Materiaux et Constructions, 42 (9), pp. 1261-1281.
3. di Prisco, M., Colombo, M., Dozio, D. Fibre-reinforced concrete in fib Model Code 2010: Principles, models and test validation (2013) Structural Concrete, 14 (4), pp. 342-361.
4. European Committee for Standardization, *EN 14651 (*2005) *Test method for metallic fibered concrete - Measuring the flexural tensile strength (limit of proportionality (LOP), residual),* p. 17.
5. Fédération Internationale du Béton (fib), (2013) *fib Model Code for Concrete Structures 2010*, Berlin (Germany): Wilhelm Ernst und Sohn Verlag für Architektur. 402.
6. Ferrara, L., di Prisco, M. (2001) Three-vs. four-point bend tests: a numerical investigation on plain concrete, Studi e ricerche,-Politecnico di Milano. Scuola di specializzazione in costruzioni in cemento armato, Italcementi, 22, pp.73-119.